3D calculation for the alignment of LHC low-beta quadrupoles

V. Rude, A. Herty, G. Kautzmann, H. Mainaud Durand, A. V. Naegely, M. Sosin, M. Udzik,
CERN, Geneva, Switzerland

Abstract

The low beta triplet quadrupoles magnets of the Large Hadron Collider (LHC) are located on both sides of the ATLAS, CMS, ALICE and LHCb experiments. The alignment tolerances of these components are particularly stringent with ±0.5 mm at 3σ and are tracked by an alignment system consisting of micrometric sensors and motorized jacks used for components remote adjustment. The system has been installed in 2008 with the purpose of monitoring the triplets relative displacements with respect to their nominal position. After the development of appropriate calibration benches, the first absolute calibrations of the sensors have been performed in 2016, allowing a determination of the magnet positions in an absolute reference frame. The radial and vertical (plus roll) data were separated in two different calculations steps.

During the LHC Long Shutdown 2 (LS2, 2019-2021), consolidation works have been carried out on all triplets allowing to perform absolute calculation in 3D, and significantly increasing the position determination accuracy. This paper gives an overview of the 3D calculations used currently for the alignment of low beta quadrupoles magnets and summarizes their positions change since LS2.

INTRODUCTION

The low beta quadrupoles (Q1, Q2, and Q3) are located on each side of the four main LHC experiments [1] (Fig. 1). Their location, in high-level radiation area, makes them particularly difficult to align. The requested alignment tolerances for the low beta quadrupoles (left and right) are ±0.5 mm at 3σ with respect to nominal position.

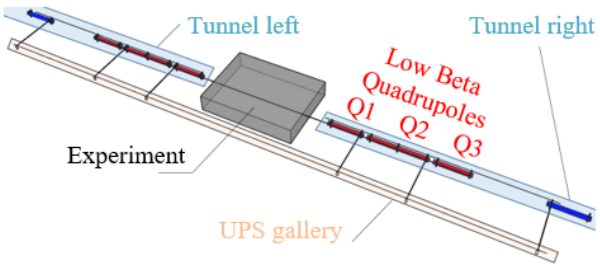

Figure 1: LHC low-beta configuration.

The low beta quadrupoles of the LHC are equipped with permanent position monitoring sensors, described hereafter. The absolute position of the quadrupoles is determined based on the sensor measurements, .

The main objective of the present contribution is to explain the 3D calculation used for the position determination. In the first part of the paper, the permanent instrumentation is described. In the second part, the 3D calculation is detailed as well as the results for the low beta quadrupoles installed around ATLAS. Finally, the perspectives of 3D calculation for new projects at CERN are addressed.

QUADRUPOLES SURVEY EQUIPMENT

The position of each cryostat is monitored according to 5 degrees-of-freedom, thanks to a combination of three alignment systems: the Wire Positioning System (WPS), the Hydrostatic Levelling System (HLS) and the Distance Offset Measurement Sensor (DOMS) [2].

For ATLAS and CMS experiments, the alignment between low beta quadrupoles on the left and right side of the experiments, is carried out thanks to radial measurements of on invar rods installed perpendicular to the tunnel [3] (Fig. 2). Six rods are installed on both sides of ATLAS and CMS experiments with respective lengths of 16 m and 11 m. DOMS sensors installed on components (quadrupoles and dipole) measure the positions of the extremities of the invar rod. The other extremities of invar rods are monitored by a DOMS installed on six different plates inside a parallel tunnel named UPS gallery.

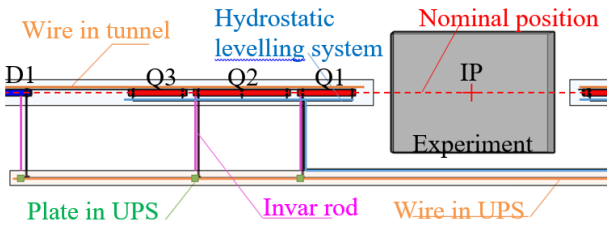

Figure 2: Survey equipment on low beta quadrupoles (top view)

A 126 m long wire is stretched in the UPS galleries and measured by six WPS installed on these six different plates. Another wire, 40 m long, is stretched on each side between Q1 and D1 (dipole 1). Each WPS, fixed to an interface installed on the quadrupole, measures the position of the wire on its interface.

HLS installed on the quadrupoles between Q3 Left and Q3 Right observe several water networks to cope with the tunnel slope.

Fig. 3 shows the position of sensors on the low beta quadrupoles.

CERN-BE-2023-003
31/10/2022

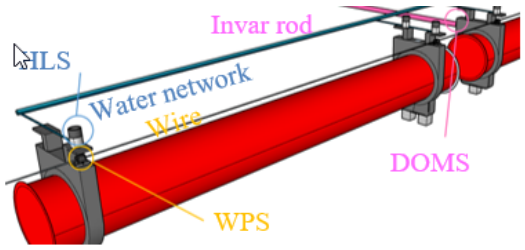

Figure 3: Sensors position on low beta quadrupoles.

PREVIOUS CALCULATION METHOD

The survey equipment has been installed in 2008 aiming to monitor the relative displacements of components with respect to the initial alignment done with classical topographical instrumentation (total station, precise levelling system) [4]. When the deviations to the initial alignment became too significant, a remote adjustment was performed by moving high precision jacks installed under each low beta quadrupole. The positions of the WPS were assumed to be horizontal. Therefore, the first reading of the WPS was assimilated to radial displacement while the second reading was related to vertical displacement. Similarly, the DOMS readings on the invar rods and the HLS readings were respectively considered horizontal and vertical.

In 2016, the first absolute sensor calibrations have been performed. The positions of the wire, water and invar rod are determined in the coordinate system of a mechanical interface. For the WPS, an isostatic interface based on three reference spheres is used. For the HLS, the top plane of the vessel is used. During the fiducialisation process, the positions of these interfaces with respect to the axis of the magnet are deduced. Thanks to this calibration and the fiducialisation, it is possible to compute the magnet positions in an absolute reference frame. The radial and vertical (plus roll) data continued to be separated in two different calculations steps [5]. This calculation does not take in account the rotation of the supports, considered as negligible, which is far from being the case when alignment tolerances are as stringent as for the low beta quadrupoles.

3D CALCULATION

Since 2019 each sensor installed in the LHC (WPS, HLS or DOMS) is calibrated in absolute and installed on an interface, allowing micrometric repeatability of sensor installation [6]. These interfaces are fixed on the components and can be characterised by a coordinate system (Fig. 4).

Fiducialisation and calibration process

During the fiducialisation process, the transformation from R-interface to R-component can be deducted with three translations (τ) and a rotation matrix (ρ):

$$M_{\text{R component}} = \tau + \rho \cdot M_{\text{R interface}} \quad (1)$$

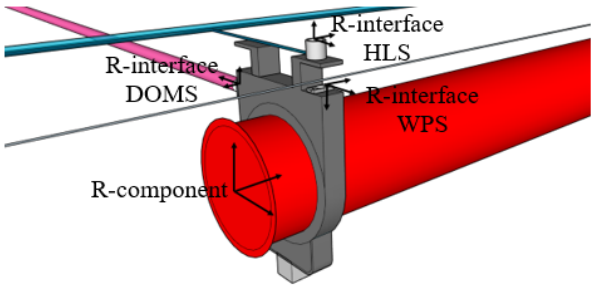

Figure 4: Coordinate systems in reference frame R-component.

During the calibration process, a polynomial function is calculated to determine:

- the position of the wire in R-interface-WPS
- the position of the water in R-interface-HLS
- the position of the extremity of the invar rod in R-interface-DOMS.

Thanks to the fiducialisation and calibration process, it is possible to determine the position of the wire, of the water and of the invar rod in the coordinate system of each quadrupole (Fig. 5).

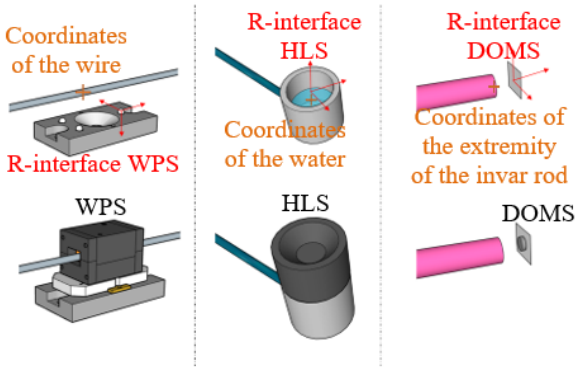

Figure 5: Observations in R-interface.

The wires, water networks and invar rods will allow the position determination of the different quadrupoles in a common coordinate system.

3D Transformation for components

The position of each cryostat must be defined in the CERN Coordinate System (CCS) [7].

For a better understanding, a local coordinate system (R-local) has been defined for each experiment by constant parameters (azimuth of the vertical plane containing the nominal beam axis) (Fig. 6).

$$M_{\text{R general}} = T + R \cdot M_{\text{R local}} \quad (2)$$

with T, R as constant parameters.

Therefore, in R-local, the position of each cryostat will be determined by five unknown parameters:

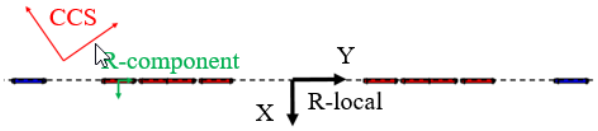

Figure 6: 3D Transformations.

- Radial translation (t_X)
- Vertical translation (t_Z)
- Pitch angle (θ_X)
- roll angle (θ_Y)
- Yaw angle (θ_Z)

$$M_{\text{R local}} = t + r \cdot M_{\text{R component}} \tag{3}$$

with

$$t = \begin{bmatrix} t_x \\ t_y \\ t_z \end{bmatrix} \quad \text{and} \quad r = r \cdot r_{\theta z} \cdot r_{\theta y} \cdot r_{\theta x}$$

Stretched Wire model

A stretched wire can be modelled by a straight line on horizontal plane and a catenary in the vertical direction (Fig. 7) that can be linearized by a second order polynomial [8].

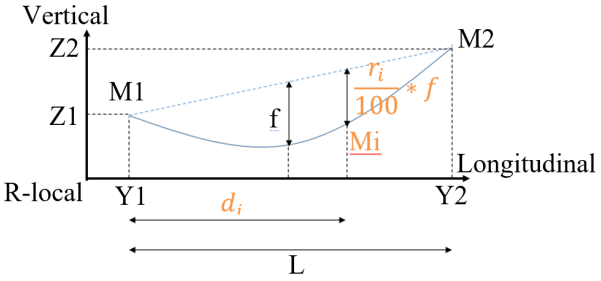

Figure 7: Stretched wire model.

$$M_i = M_1 + \frac{d_i}{L} \cdot (M_2 - M_1) - \frac{r_i}{100} \cdot f \tag{4}$$

For each wire, a local coordinate system has been defined to model the stretched wire. The transformation from local coordinate system to Rccs system is defined by constant parameters (azimuth of the vertical plane containing the nominal beam axis).

In the local coordinate system (R-local), the wire is modelled by five unknown parameters:

- Radial and vertical coordinates of extremity 1 (X_{M1} and Z_{M1}),
- radial and vertical coordinates of extremity 2 (X_{M2} and Z_{M2}),
- wire of the sag (f).

The longitudinal coordinates of the extremities of the wire, the length of the wire and for each WPS the distance to the beginning of the wire (Y_{M1},Y_{M2}, L and d_i) are known with a precision better than a few millimetres (through laser tracker measurements), which is sufficient. In addition, for each WPS, the ratio of the sag can be considered as constant ($\frac{r_i}{100}$). This ratio will notably be 100 % for the WPS installed in the middle of the wire and 0 % for the extremities. The formula below has been used to calculate the ratio of sag for each WPS:

$$\frac{r_i}{100} = \frac{\frac{4 \cdot f \cdot d_i^2}{L^2} - \frac{4 \cdot f \cdot d_i}{L}}{f} \tag{5}$$

with f as the theoretical sag of the wire $f = \frac{(g \cdot q \cdot L^2)}{8 \cdot T}$, with the acceleration of the gravity , g, the theoretical linear mass of wire, q and the theoretical tension of wire, T.

Hydrostatic surface model

The water follows a hydrostatic equilibrium whose geometry is an equipotential surface of the Earth's gravity field (Fig. 8). The model of the geoid is needed.

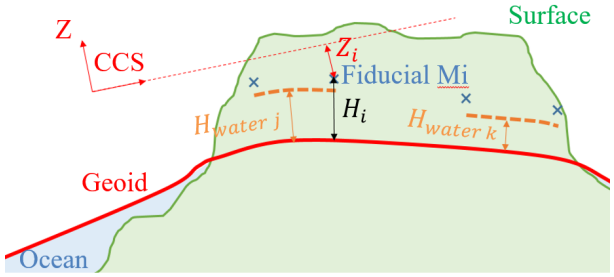

Figure 8: Hydrostatic surface model.

$$M_{\text{iRccs}} = \begin{bmatrix} X_i \\ Y_i \\ H_{\text{water j}} + \Delta(Z_i - H_i) \end{bmatrix} \tag{6}$$

X_i, Y_i, Z_i and H_i come from the approximate coordinate of the fiducial M_i, given by the determination of the geoid in Rccs. For each HLS, the nominal difference $(Z_i - H_i)$ at the level of the fiducial M_i and at the level of the water H_{water} might be considered similar and constant. The H coordinate represents the height of geoid CG1985 defined in 1985 in the tunnel [9]. For each water network, the H of the water is identical for all the HLS installed on this network. It is an unknown parameter.

Invar rod model

The invar rods were installed and measured in 2008. They are installed inside a supporting profile and suspended on a cable railway positioned in the LHC boreholes (Fig. 9). During the LS2, their lengths and their orientations have been controlled. Some differences up to 0.3 mm have been observed.

$$M_{2\,\text{local}} - M_{1\,\text{local}} = L_{\text{invar rod}} \tag{7}$$

with $M_{1\,\text{R local}} = t_1 + r_1 \cdot M_{\text{R component}}$
and $M_{2\,\text{R local}} = t_2 + r_2 \cdot M_{\text{R plate}}$

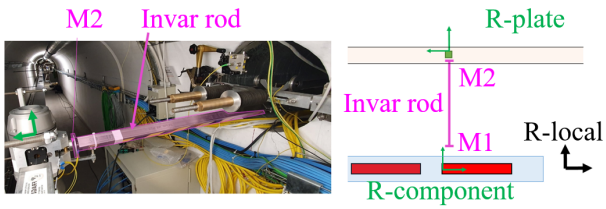

Figure 9: Invar rod model.

Equations of observations for WPS

The observations of the WPS in R-local can be deduced from 3D transformations and from the stretched wire mode, resulting in:

$$M_{\mathrm{R_{WPS}}} = \rho^{\mathrm{T}}\left[r^{\mathrm{T}}\cdot\left(M_1+\frac{d_{\mathrm{i}}}{L}\cdot(M_2-M_1)-\frac{r_{\mathrm{i}}}{100}\cdot f-t\right)-\tau\right] \quad (8)$$

with $\tau, \rho, d_{\mathrm{i}}, L, r_{\mathrm{i}}$ as constant
and t, r, M_1, M_2, f as unknown parameters.

The standard deviation of the WPS observations can be obtained from the standard deviations of the fiducialisation, the calibration and the model. An a-priori precision of 0.03 mm has been defined.

Equations of observations for HLS

The observations of the HLS in R-ccs can be deduced from 3D transformations and from the hydrostatic surface mode, resulting in:

$$M_{\mathrm{R_{HLS}}} = \rho^{\mathrm{T}}\cdot\left\{r^{\mathrm{T}}\left[R^{\mathrm{T}}\cdot\left(M_{\mathrm{iR_{general}}}-T\right)-t\right]-\tau\right\} \quad (9)$$

with $\tau, \rho, T, R, X, Y, \Delta(Z-H)$ as constant
and t, r, H_{i} as unknown parameters

An a-priori precision of 0.03 mm has been defined for the HLS observations.

Equations of observations for DOMS

The observations of the DOMS in R-local can be deduced from 3D transformations and from the invar bar model, resulting in:

$$r2\cdot\rho2\cdot M2_{\mathrm{R_{DOMS}}} - r1\cdot\rho1\cdot M2_{\mathrm{R_{DOMS}}} = L_{\text{invar rod}} - t2 + t1 - r2\cdot\tau2 + r2\cdot\tau1 \quad (10)$$

with $\tau1, \rho1, \tau2, \rho2$, and $L_{\text{invar rod}}$ as constant
and $t1, r1, t2$ and $r2$ as unknown parameters

An a-priori precision of 0.100 mm has been defined, taking into account the uncertainties of the invar rods length and the fiducialisation.

Final adjustment

The positions of the two plates installed at the extremities of UPS galleries are fixed to their last measurements in Rccs. Similarly, the vertical position of one pillar in each experiment, is fixed with respect to the last levelling performed from LHC deep references. These reference points are measured once a year during each YETS (Year End Technical Stop) at CERN and define the position of nominal position of the beam.

RESULTS

The final positions of the components are obtained by least-square adjustment. The estimated variance factor (S_0) can be computed with the equation:

$$S_0 = \sqrt{\frac{v^T\cdot p\cdot v}{n-m}} = 0.8 \quad (11)$$

A value of 0.8 is obtained, validating at a 95 %-confident level the stochastic model and the standard deviations of the observations. The estimated standard deviations of the 3D transformations between R-component to R-local are indicated in Table 1 and show a position determination with an accuracy better that 0.1 mm.

Table 1: Accuracy of the five Degrees of freedom.

	σ Tx mm radial	σ Tz mm vertical	σ θx mrad pitch	σ θy mrad roll	σ θz mrad yaw
Q1	± 0.100	± 0.045	± 0.008	± 0.048	± 0.012
Q2	± 0.074	± 0.047	± 0.004	± 0.045	± 0.006
Q3	± 0.087	± 0.067	± 0.008	± 0.046	± 0.011

Fig. 10 shows the positions of the low beta quadrupoles on both sides of ATLAS experiment, before and after the realignment. The alignment has been carried out by remote intervention using the motorized jacks installed on each low beta quadrupoles.

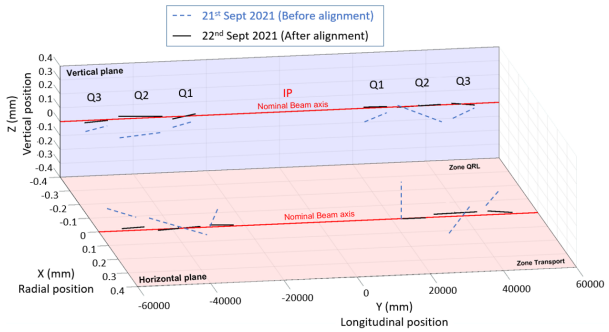

Figure 10: Alignment results (Low beta ATLAS).

LONG TERM MONITORING RESULTS

Since the LS2, the monitoring of the LHC low beta quadrupoles is performed in 3D. Fig. 11 shows the estimated variance factor (S_0) since August 2020 which stays below 1 until today. This confirms the effective functioning of the sensors WPS, HLS and DOMS.

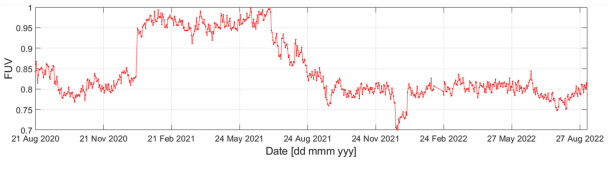

Figure 11: Estimated variance factor.

Follow-up of stretching wire (sag)

Fig. 12 shows the value of the sag of the wire installed between Q1 and D1 in the LHC tunnel (left side of the experiment) since August 2020. Some variations up to 30 µm are visible and can be explained by the variation of humidity in the LHC. The absolute value of the sag is given with an accuracy of 40 µm.

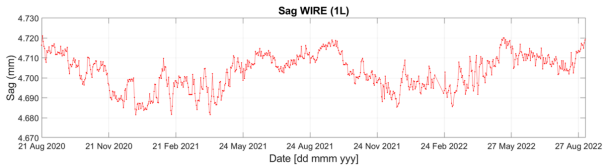

Figure 12: Sag value of wire 1Left.

Follow-up of Hydrostatic surface (H water)

Fig. 13 indicates the height of the water network installed between the experiment and tunnel 1 Left. A slope of 1 mm by year is visible and corresponds to the evaporation of the water contained in the water network. At the end of year 2021, the water network has been refilled. This operation can be done remotely thanks to an adjustable position water-tank installed on each side of the experiment and connected to water networks by gravity. The absolute value of the height is given with an accuracy of 30 µm.

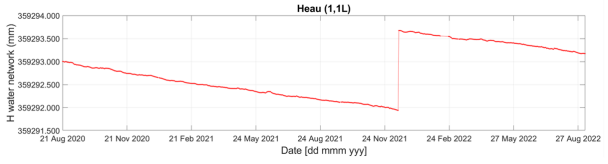

Figure 13: Height of the water (Water network 1Left).

Follow-up of positions of plates in UPS gallery

Among the six plates installed in the 126 m long UPS gallery, the two extremities plates are considered fixed in the 3D calculation. Fig. 14 shows the radial relative movement of the four plates with respected to the two extremities and suggests seasonal movements. The relative movement of the plates installed in UPS gallery is given with a precision of few micrometers.

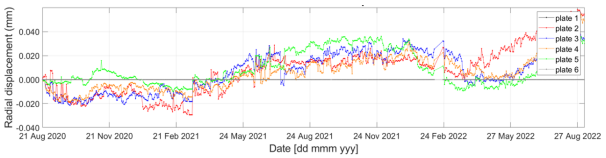

Figure 14: Radial relative movement of the plates installed in UPS Gallery.

Follow-up of 3D positions of component

Fig. 15 shows the vertical deviation from the nominal position since August 2020. Fig. 16 shows the temperature inside the cryogenic line into the components. Different steps are clearly identified:

- End of November 2020: Test on the cryogenic line. The temperature fell down from 300 K to 200 K before returning to 300 K. This led to some displacements on the triplet, in particular to a roll angle change of 20 µrad and vertical displacements up to 50 µm on Q1 Left.
- February 2021: The temperature dropped from 300 K to 1.9 K in 1 month, resulting in a variation of 150 µrad on the roll angle.
- September 2021: Alignment of the low beta quadrupoles

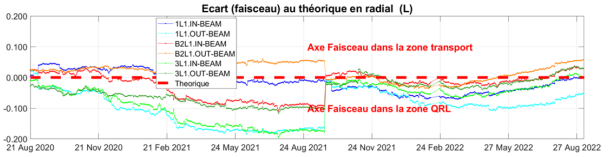

Figure 15: Vertical deviation to nominal position (1 Left).

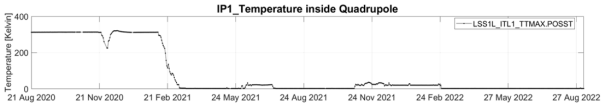

Figure 16: Temperature inside component (in Kelvin).

PERSPECTIVES

In 2026, the LHC low beta quadrupoles around ATLAS and CMS will be dismounted, as well as all the components between Q5 left to Q5 right. In total, 1.2 km of accelerator components in the Long Straight Sections (LSS) will be replaced with the objective to increase the integrated luminosity of the Large Hadron Collider (HL-LHC project) by a factor of 10 with respect to its original design

[10]. The alignment of HL-LHC LSS components will be performed by the Full Remote Alignment System (FRAS) [11], with the objective to adjust all the components between Q5 left to Q5 right in the transversal directions with an accuracy better than 150 µm.

The FRAS will consist of permanent monitoring and remote alignment systems that will cover the main components from Q1 to Q5 on each side of the experiment. To achieve the alignment tolerance, the accuracy of the sensors will be improved for the HL-LHC project. Table 2 compares the total uncertainty of each sensor, including the uncertainties of the calibration of the sensor, the models and the fiducialisation, for HL-LHC project and LHC project (actual).

Moreover, the internal monitoring will be required for HL-LHC low beta quadrupoles. It consists in measuring the position of the cold mass inside the vacuum vessel thanks to absolute distance measurements [12].

Table 2: Sensors Uncertainty for HL-LHC project.

sensors	total uncertainty for	
	HL-LHC project	**LHC project**
Long range FSI (link UPS-tunnel)	40 µm	100 µm
WPS	20 µm	30 µm
HLS	20 µm	30 µm
inclinometer	100 µrad	–
Longitudinal monitoring	300 µm	- - -
Internal monitoring	20 µm	–

The upgrade will also increase radiation levels of the Low Beta's area. Therefore, the access to the machine will be more difficult. The analysis of reliability will be a crucial point for HL-LHC. It consists of the quantification of a stochastic model to control itself. The reliability indicators state the impact on the parameters of errors that are non detectable. For example, in the LHC project, the roll angle is computed from only two HLS. It is not possible to detect any error on the observations. The local reliability of these observations are not controlled (indicator =0).

CONCLUSION

For the HL-LHC project, the 3D calculation will be necessary to achieve the required accuracy. The rotations of the supports must be taken into account and the observations of the sensors shall not be separate in two different calculations. The experience gained from 3D calculations on the LHC project will be beneficial to HL-LHC project. This calculation is currently being carried out by MATLAB external scripts. Thanks to very good results, of the 3D monitoring of LHC low-beta, the same type of calculations are foreseen to be implemented within the control system algorithms for HL-LHC FRAS.

REFERENCES

[1] W. Coosemans et al., *The alignment of the LHC Low Beta Triplets: Review of instrumentation and methods*. 7th International Workshop on Accelerator Alignment, SPring-8, Japan, 2002.

[2] A. Herty, *Micron precision calibration methods for alignment sensors in particle accelerators*. Master thesis, Nottingham Trent University, United Kingdom, 2009.

[3] H. Mainaud Durand et al., *Status of the alignment of the LHC Low Beta quadrupoles*. 8th International Workshop on Accelerator Alignment, CERN, Geneva, Switzerland, 2004.

[4] H. Mainaud Durand et al., *Permanent monitoring of the LHC Low beta triplets: latest results and perspectives*. 11th International Workshop on Accelerator Alignment, DESY Hamburg, Germany, 2010.

[5] A. Herty, *High accuracy continuous position determination of large accelerator components*. EUSPEN, CERN, Geneva, Switzerland, 2020.

[6] T. Touzé, *Proposition d'une méthode d'alignement de l'accélérateur linéaire CLIC*. Thèse de doctorat, Université de Paris-Est, Marne la vallée, France, 2011.

[7] M. Jones, *Beamline element definitions with conventions and derivations*.EDMS 1476360, CERN, Geneva, Switzerland, 2014.

[8] H. Mainaud, *Une nouvelle approche métrologique: l'écartométrie biaxiale. Application à l'alignement des accélérateurs de particules*. Thèse de doctorat, Université Louis Pasteur, Strasbourg, France, 1996.

[9] M. Jones et.al., *Geodetic parameterisation of tghe CNSG project*. International Workshop on Accelerator Alignment, SPring-8, Japan, 2002.

[10] I. Béjar Alonso et al. (ed.), *High-Luminosity Large Hadron Collider (HL-LHC): Technical design report*, CERN, CERN Yellow Reports: Monographs, 2020. https://doi.org/10.23731/CYRM-2020-0010

[11] A. Herty et.al., *HL-LHC Full Remote Alignment Study*. IPAC, Melbourne, Australia, 2019.

[12] V. Rude, *Multi-target frequency scanning interferometry to determine the position of components inside a vessel at a cryogenic temperature*. EUSPEN, CERN, Geneva, Switzerland, 2020.